

		ISSN 0016-7037 Volume 73, Number 10 May 15, 2009			
Geochimica et Cosmochimica Acta JOURNAL OF THE GEOCHEMICAL SOCIETY AND THE METEORITICAL SOCIETY					
Executive Editor: FRANK A. PODOSEK	Editorial Manager: LINDA TROWER Editorial Assistant: KATHY KLEIN KATHY SEEVER	Webmaster: ROBERT H. NICHOLS, JR. Production Manager: CHRIS ANGER			
Associate Editors:	ROBERT C. ALLEN BRIFFY G. ALT YURI AMELIN CAROL ANGETTI MAYUMI BAR-MATTHEWS LARRY G. BENDIS THOMAS S. BRANON JAY A. BRANSON ALAN D. BRANSON DAVID J. BRONKHORST ROBERT H. BURSE WILLIAM H. CAHILL THOMAS CHAPPEL JON CHAPMAN ANNE COHEN DAVID R. COLE	CHRISTOPHER DAGGNEY ZARINNO D'AVAN JAMES FARQUHAR FREDERICK A. FREY SUSAN GAEDER JENNIFER N. GOSWAMI JONAS R. HAAS H. ROBERT HANCOCK GEORGE R. HILL STACY R. HINSHAW GEORGE F. HURD JERRY HURTA TREVOR IRVING JUN-ICHIRO ITOHASHI KAREN JOHANNESSEN CLARK JOHNSON	CHRISTIAN KORBEL RONNY KUBERTY STEFAN M. KRAMER S. KRISHNAMURTHY ALEXANDER N. KRÖTZ JAMES KUBICKI GRIHAM A. LAGAN TIMOTHY J. LYONS MICHAEL L. MACTHERY BERNARD MAREY TOM MCCOLLUM ANDREW MORGAN MARTIN A. MÜNSTER JACK J. MURPHY ALONSO MATEI BOB MASON	HIDEO NAGAIWA MARTIN NIKOLIC PEGGY A. O'DAY ERIC H. OELKERS DIMITRI PAPANASTASIOU SANDRO PIZZAGALLI MARK REIKAMPER W. UWE RIMMOLD EDWARD M. RIPLEY KEVIN ROBERTS J. KELLY RUSSELL SARA S. RUSSELL F. J. RYBISON JACQUES SEWETZ JEFFREY SHAWALD TIMOTHY J. SHAW	J. S. SPRONK DONALD L. SPICER DIMITRI A. STRENSKY MICHAEL J. TUREK PETER ULMER DAVID J. VAUGHAN RICHARD J. WALKER LESLIE A. WALKER JOSEF WANG RON A. WOGELER CHEN ZHU
Volume 73, Number 10			May 15, 2009		
Articles					
N. ESTRADE, J. CARRIGAN, J. E. SONKE, O. F. X. DONARD: Mercury isotope fractionation during liquid-vapor evaporation experiments			2693		
D. JOUQUOT, A. REVIL, P. LEROY: Diffusion of ionic tracers in the Callovo-Oxfordian clay-rock using the Donnan equilibrium model and the formation factor			2712		
Y. TANG, R. J. REEDER: Uranyl and arsenate sorption on aluminum oxide surface			2727		
B. J. CAMPBELL, C. LI, A. L. SESSIONS, D. L. VALENTINE: Hydrogen isotopic fractionation in lipid biosynthesis by <i>H₂-consuming Desulfobacterium autotrophicum</i>			2744		
C. J. MILLER, A. L. ROSE, T. D. WATTE: Impact of natural organic matter on H ₂ O ₂ -mediated oxidation of Fe(II) in a simulated freshwater system			2758		
A. F. WHITE, M. S. SCHULZ, D. A. STONESTROM, D. V. VIVIT, J. FITZPATRICK, T. D. BULLEN, K. MAHER, A. E. BLUM: Chemical weathering of a marine terrace chronosequence, Santa Cruz, California. Part II: Solute profiles, gradients and the comparisons of contemporary and long-term weathering rates			2769		
K. MAHER, C. I. STEFFEL, A. F. WHITE, D. A. STONESTROM: The role of reaction affinity and secondary minerals in regulating chemical weathering rates at the Santa Cruz Soil Chronosequence, California			2804		
L. ZHANG, A. LUTTIG: Theoretical approach to evaluating plagioclase dissolution mechanisms			2832		
P. M. FOX, J. A. DAVIS, G. W. LUTHER III: The kinetics of iodide oxidation by the manganese oxide mineral birnessite			2850		
G. W. GREENE, K. KRISTIANSEN, E. E. MEYER, J. R. BOLES, J. N. ISRAELACHVILI: Role of electrochemical reactions in pressure solution			2862		
A. M. JONES, A. N. PHAM, R. N. COLLINS, T. D. WATTE: Dissociation kinetics of Fe(III)- and Al(III)-natural organic matter complexes at pH 6.0 and 8.0 and 25 °C			2875		
<i>Continued on outside back cover</i>					

This article appeared in a journal published by Elsevier. The attached copy is furnished to the author for internal non-commercial research and education use, including for instruction at the authors institution and sharing with colleagues.

Other uses, including reproduction and distribution, or selling or licensing copies, or posting to personal, institutional or third party websites are prohibited.

In most cases authors are permitted to post their version of the article (e.g. in Word or Tex form) to their personal website or institutional repository. Authors requiring further information regarding Elsevier's archiving and manuscript policies are encouraged to visit:

<http://www.elsevier.com/copyright>



Barium partitioning in coccoliths of *Emiliana huxleyi*

Gerald Langer^{a,b,*}, Gernot Nehrke^b, Silke Thoms^b, Heather Stoll^c

^aICTA, Autonomous University of Barcelona (UAB), 08193 Bellaterra, Spain

^bAlfred Wegener Institute for Polar and Marine Research, 27570 Bremerhaven, Germany

^cDepartment of Geology, University of Oviedo, 33005 Oviedo, Spain

Received 24 July 2008; accepted in revised form 16 February 2009; available online 4 March 2009

Abstract

The coccolithophore *Emiliana huxleyi* was grown in seawater under different Ba concentrations. The relationship of coccolith Ba/Ca ratio and seawater Ba/Ca ratio was found to be linear. The linear regression yields the apparent Ba exchange coefficient of 0.10. Our data support a recently proposed generic model (Langer G., Gussone N., Nehrke G., Riebesell U., Eisenhauer A., Kuhnert H., Rost B., Trimborn S., and Thoms S. (2006) Coccolith strontium to calcium ratios in *Emiliana huxleyi*: the dependence on seawater strontium and calcium concentrations. *Limnol. Oceanogr.* **51**, 310–320.) developed for explaining apparent exchange coefficients of metabolically inert divalent trace metals, such as Sr, in *E. huxleyi*. This model represents the first approach combining cell physiological processes and data from inorganic precipitation experiments, which quantitatively explains coccolith apparent Sr and Ba exchange coefficients.

© 2009 Elsevier Ltd. All rights reserved.

1. INTRODUCTION

The Sr/Ca ratio of coccoliths has been used in the framework of climate reconstruction as a paleo-proxy for coccolithophore growth and calcification rate for almost a decade (Stoll and Schrag, 2000). The robustness of this, and any other, proxy depends on the degree to which the underlying processes are understood. The rate dependence of the Sr exchange coefficient as determined from inorganic calcite precipitation experiments was used to explain the apparent Sr exchange coefficients of biogenic calcite (Carpenter and Lohmann, 1992). The trace metal exchange coefficient of biogenic calcite is termed apparent exchange coefficient, because the trace metal to calcium ratio of the solution from which the crystal is precipitated (at the site of calcification within the organism) is unknown (Langer et al., 2006). A subsequent study, however, showed that kinetic effects are not appropriate to explain Sr partitioning in coccolithophores (Stoll et al., 2002). Therefore a generic model was developed, which explains partitioning of metabolically in-

ert divalent trace metals in *Emiliana huxleyi* without including a dependence of the apparent exchange coefficients on growth or calcification rate (Langer et al., 2006). In this study we will use the term equilibrium exchange coefficient for the exchange coefficient determined in inorganic precipitation experiments at low growth rates. It is assumed that values determined at very low growth rates are not affected by kinetic processes (Tesoriero and Pankow, 1996).

This model combines data from inorganic calcite precipitation experiments with cell physiological concepts, thus including so called vital effects (Langer et al., 2006). The model was successfully applied to results of Sr partitioning during calcification of *E. huxleyi* (Langer et al., 2006). The basic assumption of the model is that cellular Sr and Ca transport proceeds via the same route. It is assumed that cellular Ca and Sr transport commences with a channel-mediated plasmamembrane passage (Brownlee and Taylor, 2004). Typical Ca-channels do not discriminate between Ca, Sr, and Ba (Allen and Sanders, 1994). Given that Ba, Sr, and Ca take the same route inside the cell, the aforementioned model should also be applicable to Ba partitioning. Unfortunately, no data exist for Ba partitioning in coccolithophores. Therefore we conducted batch culture

* Corresponding author.

E-mail address: Gerald.Langer@awi.de (G. Langer).

Nomenclature

d	day	[Me] _v	concentration of divalent cation Sr, or Ba in the coccolith vesicle
$K_{D_{Sr}}$	equilibrium exchange coefficient for Sr	IAP	{Ba ²⁺ }{SO ₄ ²⁻ } ion activity product of the solution
$K_{D_{Ba}}$	equilibrium exchange coefficient for Ba	K	solubility product of barite
$K_{D_{Sr}}^B$	apparent exchange coefficient for Sr	Ω	barite supersaturation
$K_{D_{Ba}}^B$	apparent exchange coefficient for Ba	[Ca] _s	Ca concentration at cell surface
[Me ²⁺]	concentration of free divalent cation Sr, or Ba	[Ca] _{sat}	Ca concentration at calcite supersaturation = 1
[Me] _s	concentration of divalent cation Sr, or Ba at the cell surface	[Sr] _v	Sr concentration in the coccolith vesicle
[Me] _B	concentration of divalent cation Sr, or Ba in the bulk medium	[Ca] _v	Ca concentration in the coccolith vesicle
[Me] _{total}	total concentration of divalent cation Sr, or Ba	μ_{cocco}	cell growth rate of <i>Emiliana huxleyi</i>

experiments with *E. huxleyi* grown under different Ba/Ca ratios of seawater.

2. MATERIALS AND METHODS

2.1. Experimental setup

To reliably determine the relationship between Ba/Ca ratio of coccoliths and Ba/Ca ratio of seawater, we varied the Ba/Ca ratio of seawater over two orders of magnitude. We are aware of the fact that such high Ba/Ca ratios are not to be found in today's sea surface waters. However, to reveal the underlying mechanisms of trace metal incorporation into biogenic calcite it is often necessary to alter the physicochemical conditions beyond the range typically observed in the natural environment. An increase of natural seawater Ba concentration by a factor of 100 could lead to the precipitation of BaSO₄ (barite) (supersaturation Ω is approx. 60 ($\Omega = IAP/K$, where K is the solubility product of barite, and $IAP = \{Ba^{2+}\}\{SO_4^{2-}\}$ the ion activity product of the solution), as calculated by means of the speciation software Visual Minteq V. 2.53 (Gustafsson, 2007). For that reason, we performed test-experiments with Ba concentrations of 7 $\mu\text{mol L}^{-1}$. For reference, the Ba concentration of natural sea surface water is 0.06 $\mu\text{mol L}^{-1}$ (Wolgemuth and Broecker, 1970).

In these experiments barite precipitation could be detected as inferred from (a) lowered Ba concentration in seawater at the end of experiment and (b) crystals present in filtrated seawater showing typical barite morphology, as imaged by a scanning electron microscope (SEM). Therefore natural seawater (NSW) was only suitable for the natural Ba concentration used in the experiments, which represents the lowest concentration used in the experiments.

In order to perform culture experiments at elevated Ba concentrations, we used artificial seawater (ASW) with a sulphate concentration of 2.84 mmol L⁻¹, an order of magnitude lower sulphate concentration than natural seawater. The detailed composition of the artificial seawater is given in Table 1. Ba concentration over the course of the experiment was constant within analytical error. A monospecific culture of *E. huxleyi* (strain PML B92/11) was grown in

sterile filtered (0.2 μm) artificial seawater enriched with 100 $\mu\text{mol L}^{-1}$ nitrate and 6.25 $\mu\text{mol L}^{-1}$ phosphate with trace metals and vitamins according to F/2 (Guillard and Rytter, 1962).

A 16:8 light:dark cycle was applied. Experiments were carried out at a constant temperature of 17 °C and a constant photon flux density of 270 $\mu\text{mol photons m}^{-2} \text{s}^{-1}$, during light hours, which were maintained by growing the cells in an adjustable incubator (Rubarth Apparate GmbH, Germany). Cells were pre-adapted to experimental conditions for approximately seven generations and grown in dilute batch culture (also 7 generations, total culturing period 9 days), which ensures insignificant alteration of the carbonate system over the course of the experiment (Langer et al., 2006). CO₂ concentration was adjusted to 15.3 $\mu\text{mol L}^{-1}$ (pH 8.2) through the addition of NaOH (1 mol L⁻¹). The carbonate system was calculated from temperature, salinity, concentrations of dissolved inorganic carbon (DIC), phosphate and pH (NBS scale) using the programme CO₂sys (Lewis and Wallace, 1998). Equilibrium constants of (Mehrbach et al., 1973) refitted by (Dickson and Millero, 1987) were chosen.

The cells were grown in triplicate in 2.5 L polycarbonate flasks. Seawater samples for Ba, Sr, and Ca analyses were filtered (polycarbonate filters, 0.2 μm) and subsequently diluted (10 times) with reverse osmosis water (ROW) (conductivity 0.067 μS). Samples for measurement of coccolith

Table 1
Composition of artificial seawater.

Salt	Final concentration (mmol L ⁻¹)
NaHCO ₃	2.33
NaCl	394
MgCl ₂	53.6
Na ₂ SO ₄	2.84
KCl	10
SrCl ₂	0.09
KBr	0.84
CaCl ₂	10
H ₃ BO ₃	0.4
BaCl ₂	Variable, see Table 2

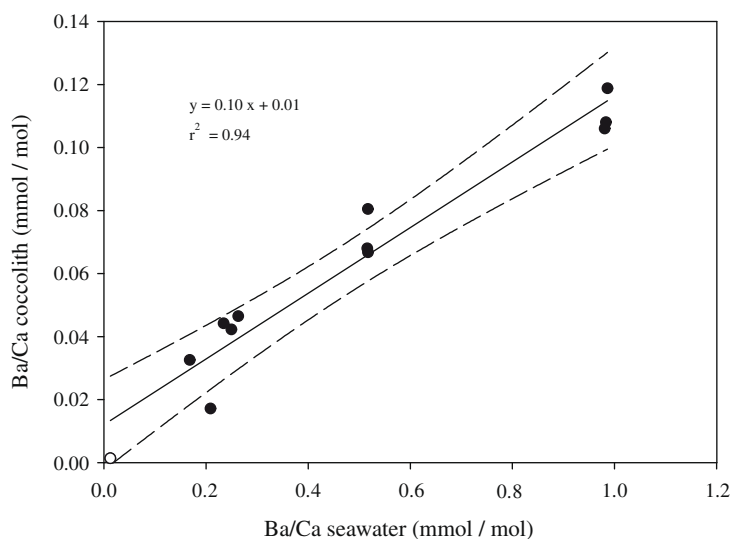


Fig. 1. The dependence of the Ba/Ca ratio in coccolith calcite on the Ba/Ca ratio in seawater. The slope of the linear regression curve yields an apparent Ba exchange coefficient of 0.10. The lowest Ba/Ca ratio of seawater represents the Ba/Ca ratio of natural seawater (open circle) whereas all other data points represent values measured in artificial seawater (closed circles).

calcium, barium, and strontium were filtered on polycarbonate filters (1.0 μm), dried at 60 $^{\circ}\text{C}$ for 12 h and subsequently stored at room temperature. For further processing of the filters see the following section.

For determination of cell density, samples were taken daily and counted immediately after sampling using a Coulter Multisizer III. Cell growth rate ($\mu_{\text{coccolith}}$, unit d^{-1}) was calculated by means of exponential regression. Growth rate in general is reported as [per day]. The most intuitive unit is [cell divisions per day] (growth rate k). However, in the coccolithophore literature, growth rate μ is usually given: $\mu = k * \ln(2)$. Calcification rate (P , $\text{pg calcite cell}^{-1} \text{d}^{-1}$) was calculated according to $P = \mu_{\text{coccolith}} * (\text{cellular calcite content})$. Cellular calcite content was calculated from coccolith calcium measurements.

2.2. Sample preparation and determination of Ba/Ca ratios

Ba/Ca ratios of media and coccoliths were analyzed using matrix-matched standards on a simultaneous dual ICP-AES (Thermo ICAP DUO 6300).

For determination of coccolith Ba/Ca ratios, polycarbonate filters were rinsed with ROW using vacuum filter holders. Organic matter was oxidized by a 30 min exposure to 4 mL of a 1:1 (volumetric) solution of 3% NaOCl and 30% H_2O_2 as described by (Bairbakhish et al., 1999), and subsequently rinsed using 30 mL of ROW. Samples on the filters were dissolved in 2% HNO_3 .

For coccoliths, Ba was measured in axial mode (455.4 nm) and Ca detection in both radial (315.8 and 317.9 nm) and axial mode (318.1 nm). Calibration was conducted off-line using the intensity ratio method described by (de Villiers et al., 2002). In this case, four standards were prepared with variable Ba/Ca ratios of 0.34–34 $\mu\text{mol/mol}$ and constant Ca concentrations. Aliquots from this standard set were uniformly diluted to provide calibration curves for various Ca concentrations. The relationship between measured Ba/Ca intensity ratio and standard Ba/

Ca mol ratios was linear and independent of the concentration of the standards from Ca 800 to 1600 ppm, and linear with a slightly lower slope at standard concentrations (Ca 300 ppm). For the standards run at 800 ppm Ca, counts on 455.4 Ba were 6.5 times higher than the 2% HNO_3 blank for the lowest standard, and 300 times higher than the blank for the highest standard. Instrumental uncertainty for our consistency standard (run at Ba concentrations $6 \times$ the 2% HNO_3 blank) is 2% rsd over 12 h run.

All samples from artificial seawater were run at concentrations from 500–750 ppm Ca, with the exception of one smaller sample run at 300 ppm Ca. The sample from natural seawater was smaller, and ran at 100 ppm Ca with and Ba counts 4.5 times those of the 2% HNO_3 blank. Consequently uncertainty on this sample is greater than for those from artificial seawater.

For coccolith Sr/Ca, sample dissolutions were diluted to contain 50–100 ppm Ca. Sr was measured in radial mode (407.7 nm) and Ca in radial mode (315.8 nm). As for Ba/Ca, calibration was done off-line using the intensity ratio method with three standards of variable Sr/Ca ratios from 0.5 to 3.0 mmol/mol and constant Ca concentrations. Standards run at 50 ppm Ca and 100 ppm Ca reveal that the concentration effect on Sr/Ca ratio is negligible within this dilution range.

3. RESULTS

The Ba/Ca ratio of coccolith calcite is linearly related to the Ba/Ca ratio of seawater (Fig. 1). The slope of the regression curve represents the apparent Ba exchange coefficient with a value of 0.10 (Fig. 1). The lowest data point represents the only one which was obtained from experiments using natural seawater. However, when omitting this data point, the slope is not altered. Deviation of the y -axis intercept from zero is due to analytical precision of the measurement.

Table 2

Experimental results. n.d. = not determined.

Experiment	Type of sea water (NSW or ASW)	Ba/Ca coccolith (mmol/mol)	Ba/Ca seawater (mmol/mol)	Ba exchange coefficient	Sr/Ca coccolith (mmol/mol)	Sr/Ca seawater (mmol/mol)	Sr exchange coefficient	Growth rate μ (per day)	Calcification rate (pg calcite/cell * day)
1	NSW	0.00	0.01	0.11	3.10	8.16	0.38	1.10	n.d
2	ASW	0.02	0.21	0.08	4.26	11.69	0.36	0.92	34
3	ASW	0.03	0.17	0.19	3.55	11.69	0.30	0.93	33
4	ASW	0.05	0.26	0.18	4.05	11.69	0.35	0.92	32
5	ASW	0.04	0.23	0.19	3.97	11.69	0.34	0.95	33
6	ASW	0.04	0.25	0.17	3.98	11.69	0.34	0.95	37
7	ASW	0.07	0.52	0.13	3.98	11.69	0.34	0.97	37
8	ASW	0.08	0.52	0.16	4.10	11.69	0.35	0.98	30
9	ASW	0.07	0.52	0.13	4.00	11.69	0.34	0.97	40
10	ASW	0.11	0.98	0.11	4.13	11.69	0.35	0.97	38
11	ASW	0.12	0.99	0.12	4.56	11.69	0.39	0.97	42
12	ASW	0.11	0.98	0.11	3.99	11.69	0.34	0.97	41

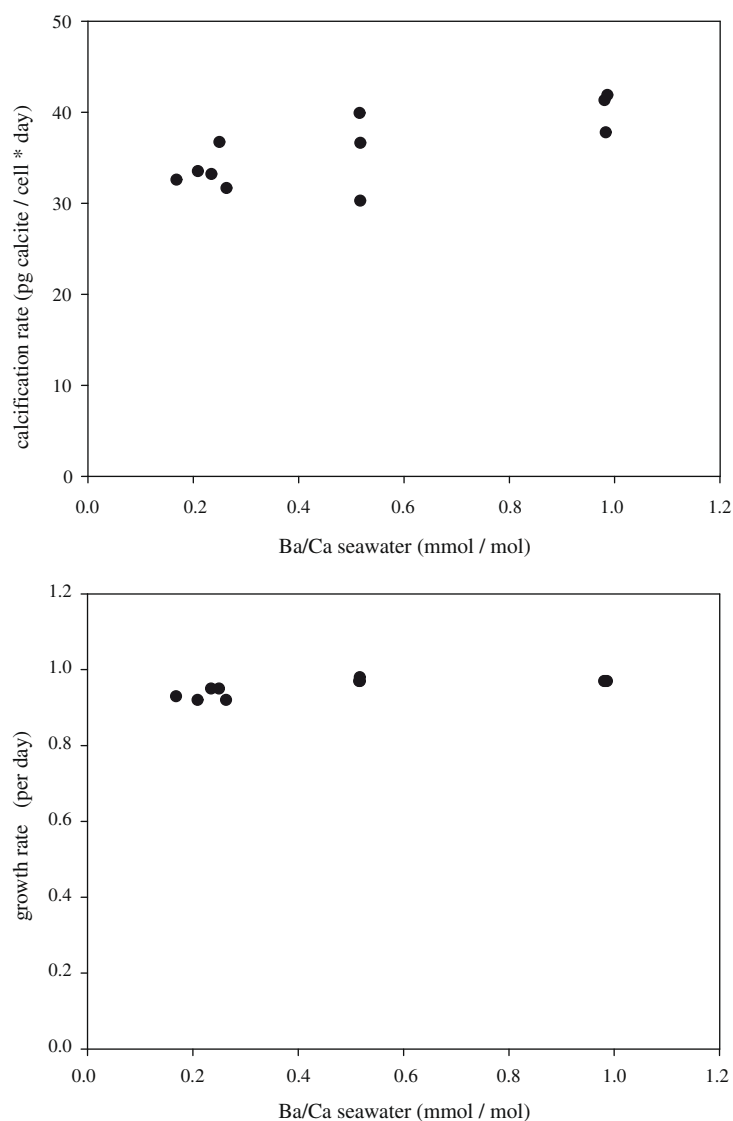


Fig. 2. The dependence of calcification rate (upper panel) and growth rate (lower panel) of *Emiliana huxleyi* on the Ba/Ca ratio of artificial seawater.

The mean apparent Sr exchange coefficient of all measured samples was 0.35, standard deviation 0.02 (Table 2).

Growth rates of cells grown in artificial seawater show negligible variability (less than 10%; lowest value divided by highest value, Fig. 2, Table 2). The variability of calcification rates (29%) is higher than the growth rate variability, but is not related to seawater Ba/Ca ratios (Fig. 2). However, neither the Ba nor the Sr apparent exchange coefficient is correlated to cell growth rates or calcification rates of *E. huxleyi* (Fig. 3).

Since it was necessary to reduce the sulphate concentration of artificial seawater to prevent barite precipitation, it was tested whether cells were sulphate limited when grown under 2.84 mmol L^{-1} sulphate (lowest concentration used in the experiments). Therefore an experiment was conducted in which the growth rate of *E. huxleyi* grown in artificial seawater under 2.84 mmol L^{-1} sulphate was

compared to the growth rate under 28.4 mmol L^{-1} (normal seawater sulphate concentration). Growth rate under 2.84 mmol L^{-1} sulphate was 0.92 ± 0.02 , as opposed to a growth rate of 1.4 ± 0.02 under 28.4 mmol L^{-1} sulphate (standard deviations were calculated from triplicate incubations), indicating sulphate limitation. Unfortunately, no data exist on the effect of sulphate limitation on trace metal incorporation in coccolith calcite. However, the natural seawater data point lies within the 95% confidence interval of the linear regression (Fig. 1), demonstrating that sulphate limitation has no significant effect on the apparent Ba exchange coefficient.

For Sr, an effect of sulphate limitation on the apparent exchange coefficient is unlikely too, since the apparent exchange coefficients calculated for the experiments using natural and artificial seawater show no significant difference (0.38 compared to 0.35 ± 0.02 , Table 2).

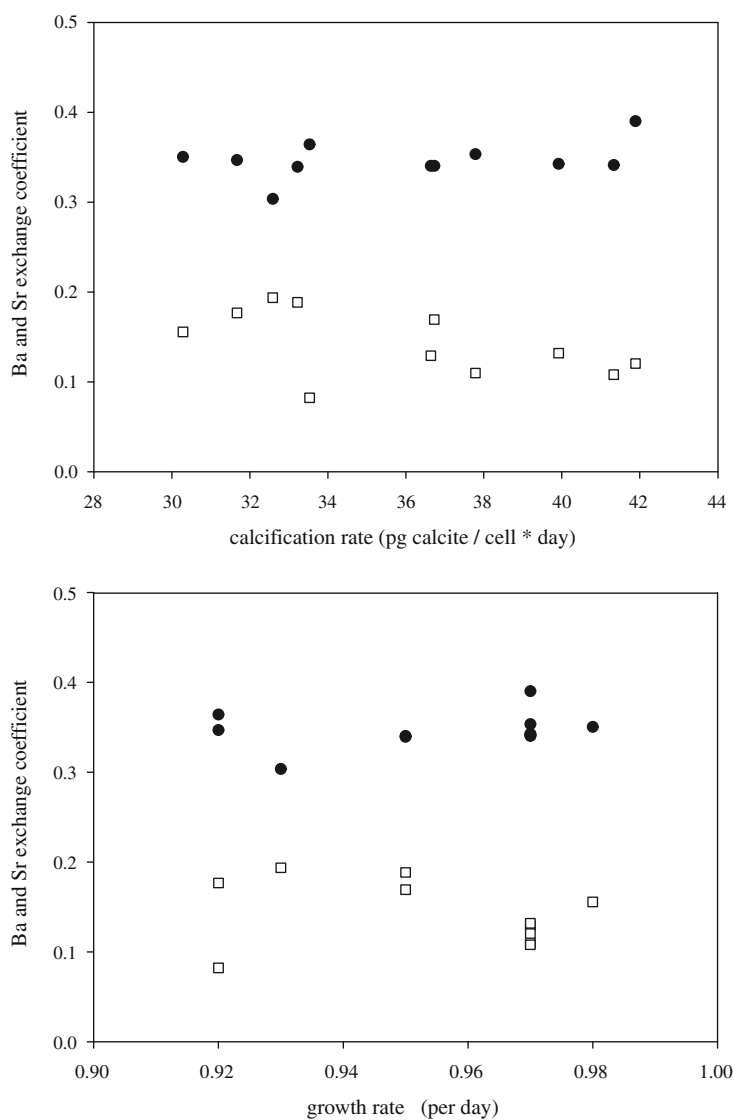


Fig. 3. The dependence of the apparent Ba (open squares) and Sr (closed circles) exchange coefficient of coccolith calcite on calcification rate (upper panel) and growth rate (lower panel) of *Emiliana huxleyi*.

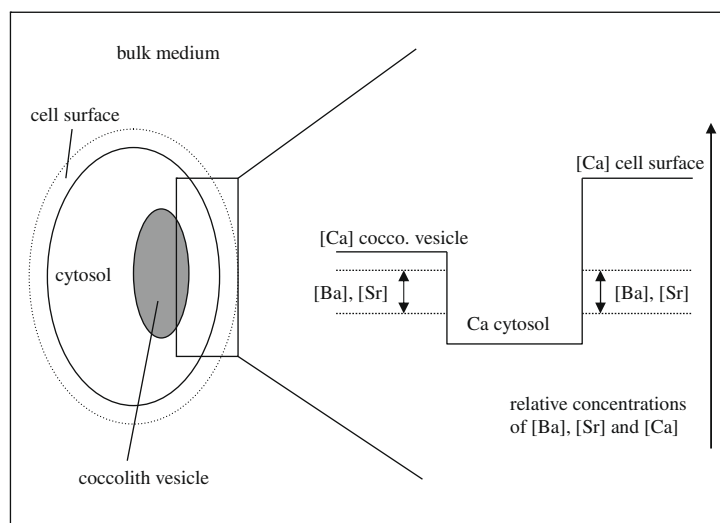


Fig. 4. Proposed mechanism for the partitioning of Sr, Ba and Ca during calcification in *Emiliana huxleyi* yielding the $K_{D_{Sr}}^B$, and $K_{D_{Ba}}^B$. Depicted are the relative concentrations of Sr, Ba, and Ca in the two involved cellular compartments (coccolith vesicle and cytosol) and the cell surface. The Sr and Ba concentrations (dashed lines) at the cell surface and in the coccolith vesicle increase until the thermodynamical limit of the concentration gradient between the cytosol and adjacent compartments is reached. The same holds for the Ca concentration (solid lines) at the cell surface. However, the Ca concentration in the coccolith vesicle is determined by the saturation product. All variations of the Sr and Ba concentrations at the cell surface are reflected by variations of the Sr and Ba concentrations in the coccolith vesicle (as indicated by the double-headed arrows).

4. DISCUSSION

The Ba exchange coefficient determined for coccoliths (0.10) is high compared to the one of inorganically precipitated calcite (0.012) (Fig. 1, Tesoriero and Pankow, 1996). The same holds true for the Sr exchange coefficient (Table 2, Nehrke et al., 2007; Tesoriero and Pankow, 1996). In a previously published study (Langer et al., 2006) it could be shown that the discrepancy between the coccolith Sr ex-

change coefficients and the respective inorganic equilibrium exchange coefficients (Tesoriero and Pankow, 1996) can be explained by a model which takes into account physiological transport processes. In the following we will first summarize the basic features of the model and then discuss the application of the model to Ba partitioning.

This model is based on the assumption that metabolically inert divalent cations are transported inside the cell via the Ca transport pathway. Since Sr and Ba can be re-

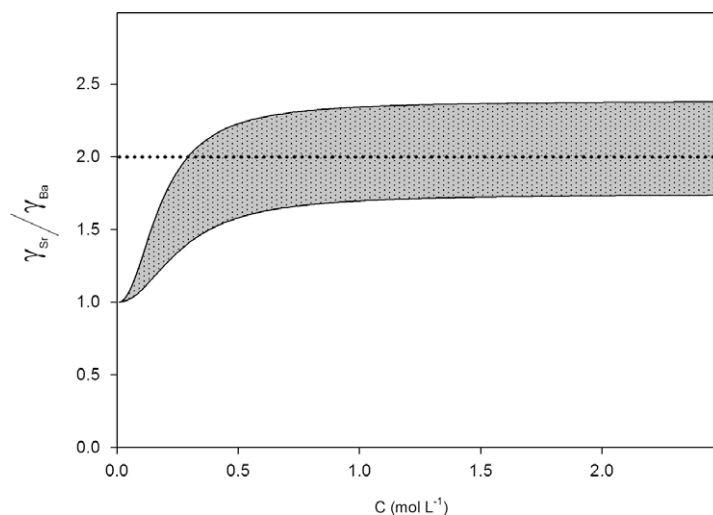


Fig. 5. Comparison of the ratio γ_{Sr}/γ_{Ba} derived from our data using Eq. (7) (dotted line) with calculated γ ratios as a function of the polysaccharide concentration C using Eq. (6). The latter includes the dissociation constants of the ion-exchange reaction K_{diss}^{Mc} (defined in Eq. (4)) which were derived from a gelation experiment with an alginate system (Yuryev et al., 1979). The K_{diss}^{Mc} values for the upper (lower) boundaries of the gelation region (gray area) are given by: $K_{diss}^{Sr} = 0.068 \pm 0.012(0.031 \pm 0.007)$ and $K_{diss}^{Ba} = 0.039 \pm 0.002(0.013 \pm 0.001)$, K_{diss}^{Mc} in mol² L⁻².

garded as metabolically inert (e.g. Salisbury and Ross, 1992), Ba can be substituted for Sr in the model. The Ca transport pathway inside the cell is comprised of Ca-channels in the plasmamembrane and Ca pumps in the endomembrane system. Neither Ca-channels nor pumps are assumed to fractionate for or against Sr. Calcite precipitation at the site of calcification (coccolith vesicle), however, fractionates against Sr (Tesoriero and Pankow, 1996). As a consequence, the Sr concentration in the fluid of the coccolith vesicle ($[Sr]_V$) rises during coccolith growth. The $[Sr]_V$ can only rise up to a maximum value, which is determined by the thermodynamical limit of the Ca pump. It should be noted that this consideration applies also to the Ca pumps in the plasmamembrane, i.e. the gradient of Sr is the same over the coccolith vesicle membrane and the plasmamembrane. According to the model, the maximum $[Sr]_V$ is reached within the first 6 seconds of coccolith growth (the time needed to precipitate a coccolith was estimated being 0.7 h).

The Ca concentration in the coccolith vesicle ($[Ca]_V$) is assumed to be close to the saturation value ($[Ca]_{Sat}$), i.e. the lowest Ca concentration which still ensures calcite precipitation. Considering the small volume of the coccolith vesicle fluid, it follows that the Sr/Ca of a coccolith is determined by the steady state concentrations of Sr and Ca. A further consequence of this mechanism is that the Sr concentration in the coccolith vesicle ($[Sr]_V$) and the Sr concentration at the cell surface ($[Sr]_S$) are similar (due to the thermodynamical limit of the Ca pumps in the coccolith vesicle membrane and the plasmamembrane, see above). Therefore, $[Sr]_V$ mirrors all changes of $[Sr]_S$. According to the model the $K_{D_{Sr}}^B$ is calculated by means of the following equation:

$$\begin{aligned} K_{D_{Sr}}^B &= K_{D_{Sr}} \frac{[Sr]_V}{[Ca]_V} \frac{[Ca]_B}{[Sr]_B} = K_{D_{Sr}} \frac{[Sr]_V}{[Ca]_{Sat}} \frac{[Ca]_S}{[Sr]_S} \\ &= K_{D_{Sr}} \frac{[Ca]_S}{[Ca]_{Sat}} = \text{const.} \end{aligned} \quad (1)$$

where $[Ca]_S$ is assumed to be seawater concentration.

It has to be noted that a small amount of polysaccharides, the so called coccolith associated polysaccharides (CAP) (Henriksen et al., 2004), is always present at the cell surface of *E. huxleyi*. Divalent cations bind to polysaccharides by a complexation mechanism called egg-box model (Braccini and Perez, 2001). The binding strength is dependent on the species of divalent cation (Me^{2+}). Although no data on binding affinities of different cations are available for CAP, such data do exist for the alginate system. In the latter case the affinity of the polysaccharides to the divalent cations increases in the series: $Ca^{2+} < Sr^{2+} < Ba^{2+}$, i.e. Ba is bound more strongly to polysaccharides than Sr (Yuryev et al., 1979). Therefore the free Sr concentration at the cell surface ($[Sr^{2+}]_S$) is reduced compared to the Sr concentration in the bulk medium ($[Sr^{2+}]_B$), an effect which is more pronounced for Ba.

The alteration of $[Me^{2+}]$ due to the binding of this divalent cation species to the polysaccharides can be described by the ratio of $[Me^{2+}]$ to the total concentration of this divalent cation, $\gamma_{Me} = [Me^{2+}]/[Me]_{total}$. Then, the effect of polysaccharides on $[Me^{2+}]$ at the cell surface is taken into

account by introducing the factor γ_{Me} ($= [Me]_S/[Me]_B$; $[Me^{2+}] = [Me]_S$ S: cell surface, $[Me]_{total} = [Me]_B$ B: bulk medium) in the equation for the apparent exchange coefficient (Eq. (1)):

$$\begin{aligned} K_{D_{Me}}^B &= K_{D_{Me}} \frac{[Me]_V}{[Ca]_V} \frac{[Ca]_B}{[Me]_B} = K_{D_{Me}} \gamma_{Me} \frac{[Me]_V}{[Ca]_{Sat}} \frac{[Ca]_S}{[Me]_S} \\ &= K_{D_{Me}} \gamma_{Me} \frac{[Ca]_S}{[Ca]_{Sat}} \end{aligned} \quad (2)$$

The factor γ_{Me} can assume values between 0 and 1. In case of no polysaccharides at the cell surface γ_{Me} equals 1.

The ratio γ_{Sr}/γ_{Ba} can be estimated from the equilibrium of the ion-exchange reaction of a sodium alginate–calcium chloride system (Yuryev et al., 1979):



where the dissociation constant is defined as:

$$K_{diss}^{Me} = \frac{[\text{RCOONa}]^2 [\text{Me}^{2+}]}{[(\text{RCOO})_2\text{Me}]} \quad (4)$$

In Eqs. (3) and (4) RCOO represents a carboxyl group of the polysaccharide backbone R.

Using the dissociation constant and the conservation law for the total concentration of the divalent ions $[Me]_{total}$:

$$[Me]_{total} = [Me^{2+}] + [(\text{RCOO})_2\text{Me}], \quad (5)$$

the following relationship for the ratio γ_{Sr}/γ_{Ba} can be derived for the alginate system:

$$\left. \frac{\gamma_{Sr}}{\gamma_{Ba}} \right|_{\text{alginate}} = \frac{[Sr^{2+}]/[Sr]_{total}}{[Ba^{2+}]/[Ba]_{total}} = \frac{K_{diss}^{Sr} (C^2 + K_{diss}^{Ba})}{K_{diss}^{Ba} (C^2 + K_{diss}^{Sr})} \quad (6)$$

where C is the concentration of the polysaccharides. For estimating the effect of CAP on the apparent exchange coefficients, the ratio γ_{Sr}/γ_{Ba} for the alginate system described by Eq. (6) is compared with the ratio γ_{Sr}/γ_{Ba} derived from Eq. (2) by using our results for the coccolith Me:Ca ratios (Table 2):

$$\left. \frac{\gamma_{Sr}}{\gamma_{Ba}} \right|_{\text{CAP}} = \frac{[Sr]_S/[Sr]_B}{[Ba]_S/[Ba]_B} = \frac{[Sr]_V/[Sr]_B}{[Ba]_V/[Ba]_B} = \frac{K_{D_{Sr}}^B/K_{D_{Sr}}}{K_{D_{Ba}}^B/K_{D_{Ba}}} \quad (7)$$

with apparent Sr exchange coefficient $K_{D_{Sr}}^B = 0.35$ (this study, Table 2), equilibrium Sr exchange coefficient $K_{D_{Sr}} = 0.021$ (Tesoriero and Pankow, 1996), apparent Ba exchange coefficient $K_{D_{Ba}}^B = 0.1$ (this study, Fig. 1), equilibrium Ba exchange coefficient $K_{D_{Ba}} = 0.012$ (Tesoriero and Pankow, 1996).

The ratio γ_{Sr}/γ_{Ba} for the alginate system (Eq. (6)) fits the ratio γ_{Sr}/γ_{Ba} for CAP (Eq. (7)) (see Fig. 3). This match supports the notion that different binding strength of Sr and Ba to CAP lead to different ratios of apparent exchange coefficient to equilibrium exchange coefficient for Ba and Sr, respectively.

To summarize, we have presented the first data on Ba partitioning of coccoliths, which show that the apparent Ba partitioning coefficient of coccoliths is firstly independent of the Ba/Ca ratio of seawater and secondly high compared to the equilibrium partitioning coefficient determined

in inorganic precipitation experiments. Assuming that CAP alters the Ba and Sr concentrations at the cell surface with respect to bulk concentrations in the way described above, than the model (Langer et al., 2006) can explain both Sr and Ba partitioning in *E. huxleyi* (see Figs. 4 and 5).

This model represents the first approach combining cell physiological processes and data from inorganic precipitation experiments, which quantitatively explains coccolith apparent Sr and Ba exchange coefficients. Explaining differences between exchange coefficients of inorganic systems and apparent exchange coefficients of biological systems is crucial to the development of a mechanistic understanding of proxies used in paleo-climate reconstruction.

ACKNOWLEDGMENTS

We thank two anonymous reviewers for their helpful comments. G. Langer acknowledges financial support by the Spanish Ministry of Science through the Juan de la Cierva programme. This work was supported by the German research foundation (DFG) under grant no. BI 432/4-2 ("PaleoSalt"), BI 432/6-1 ("BioCalc"), and TH 744/2-3 and by the European Science Foundation (ESF) under the EUROCORES Programmes EuroCLIMATE and EuroMinSci through contract No. ERAS-CT-2003-980409 of the European Commission, DG Research, FP6. We acknowledge fellowship to H. Stoll from the Spanish Ministry of Science cofunded by the European Social Fund and an instrumentation grant to H. Stoll from the Asturian Commission of Science and Technology (FICYT) cofinanced by the European Regional Development Funds. We thank M. Prieto for access to laboratory instrumentation at the University of Oviedo and for discussion.

REFERENCES

- Allen G. J. and Sanders D. (1994) Two voltage-gated, calcium release channels coreside in the vacuolar membrane of broad bean guard cells. *Plant Cell* **6**(5), 685–694.
- Bairbakhish A. N., Bollmann J., Sprengel C. and Thierstein H. R. (1999) Disintegration of aggregates and coccospheres in sediment trap samples. *Mar. Micropaleontol.* **37**(2), 219–223.
- Braccini I. and Perez S. (2001) Molecular basis of Ca²⁺-induced gelation in alginates and pectins: the egg-box model revisited. *Biomacromolecules* **2**, 1089–1096.
- Brownlee C. and Taylor A. (2004) Calcification in coccolithophores: a cellular perspective. In *Coccolithophores – From Molecular Processes to Global Impact* (eds. H. R. Thierstein and J. R. Young). Springer-Verlag, pp. 31–49.
- Carpenter S. J. and Lohmann K. C. (1992) Sr/Mg ratios of modern marine calcite: empirical indicators of ocean chemistry and precipitation rate. *Geochim. Cosmochim. Acta* **56**(5), 1837–1849.
- de Villiers S., Greaves M. and Elderfield H. (2002) An intensity ratio calibration method for the accurate determination of Mg/Ca and Sr/Ca of marine carbonates by ICP-AES. *Geochem. Geophys. Geosystems* **3**, 2001GC000169.
- Dickson A. G. and Millero F. J. (1987) A comparison of the equilibrium constants for the dissociation of carbonic acid in seawater media. *Deep-Sea Res.* **34**, 1733–1743.
- Guillard R. R. L. and Ryther J. H. (1962) Studies of marine planktonic diatoms, I. *Cyclotella nanna* (Hustedt) and *Detonula convolvacea* (Cleve). *Can. J. Microbiol.* **8**, 229–239.
- Gustafsson J. P. (2007) Visual Minteq ver. 2.53. KTH. Available from: <<http://www.lwr.kth.se/English/OurSoftware/vminteq/index.htm>>.
- Henriksen K., Stipp S. L. S., Young J. and Marsh M. E. (2004) Biological control on calcite crystallization: AFM investigation of coccolith polysaccharide function. *Am. Mineral.* **89**, 1586–1596.
- Langer G., Gussone N., Nehrke G., Riebesell U., Eisenhauer A., Kuhnert H., Rost B., Trimborn S. and Thoms S. (2006) Coccolith strontium to calcium ratios in *Emiliania huxleyi*: the dependence on seawater strontium and calcium concentrations. *Limnol. Oceanogr.* **51**, 310–320.
- Lewis E. and Wallace D. W. R. (1998) Program Developed for CO₂ System Calculations ORNL/CDIAC-105. Carbon Dioxide Information Analysis Centre, Oak Ridge National Laboratory, U.S. Department of Energy.
- Mehrbach C., Culbertson C. H., Hawley J. E. and Pytkovics R. M. (1973) Measurement of the apparent dissociation constants of carbonic acid in seawater at atmospheric pressure. *Limnol. Oceanogr.* **18**, 897–907.
- Nehrke G., Reichart G.-J., Van Cappellen P., Meile C. and Bijma J. (2007) Dependence of calcite growth rate and Sr partitioning on solution stoichiometry: Non-Kossel crystal growth. *Geochim. Cosmochim. Acta* **71**, 2240–2249.
- Salisbury F. B. and Ross C. W. (1992) *Plant Physiology*. Wadsworth Publishing Company.
- Stoll H. M., Rosenthal Y. and Falkowski P. (2002) Climate proxies from Sr/Ca of coccolith calcite: calibrations from continuous culture of *Emiliania huxleyi*. *Geochim. Cosmochim. Acta* **66**(6), 927–936.
- Stoll H. M. and Schrag D. P. (2000) Coccolith Sr/Ca as a new indicator of coccolithophorid calcification and growth rate. *Geochem. Geophys. Geosystems* **1**, 1999GC000015.
- Tesoriero A. J. and Pankow J. F. (1996) Solid solution partitioning of Sr²⁺, Ba²⁺, and Cd²⁺ to calcite. *Geochim. Cosmochim. Acta* **60**(6), 1053–1063.
- Wolgemuth K. and Broecker W. S. (1970) Barium in sea water. *Earth Planet. Sci. Lett.* **8**(5), 372–378.
- Yuryev V. P., Grinberg N. V., Braudo E. E. and Tolstoguzov V. B. (1979) A study of the boundary conditions for the gel formation of alginates of polyvalent metals. *Starch/Stärke* **4**, 121–124.

Associate editor: Jack J. Middelburg